Effect of Ag-Doping on the Photoluminescence of Nanostructered ZnS Material

Publisher: IEEE

Ana Laura Curcio ; Thiago Ardana Chaim ; Maria Inês Basso Bernardi ; Fabio Simões de Vicente ; Adriano José Galvani Otuka ; Alexandre Mesquita

All Authors

Abstract:
Zinc sulfide (ZnS) is a wide band gap semiconductor with numerous technological applications in optical devices. In this study, nanostructured Ag-doped ZnS samples were prepared by solvothermal method. Pure-ZnS sample exhibits cubic symmetry of sphalerite structure whereas samples with higher values of Ag content exhibits coexistence of sphalerite structure and wurtzite structure with hexagonal symmetry. Photoluminescence spectra present typical four emissions ascribed to Zn and S vacancies, Zn and S interstitials for ZnS host matrix. As the Ag content increases, the relative intensity increases for red-orange emissions and an additional emission is observed, allowing a tunable photoluminescence emission with Ag-doping.

Published in: 2025 SBFoton International Optics and Photonics Conference (SBFoton IOPC)

Date of Conference: 21-24 September 2025

Date Added to IEEE *Xplore*: 31 October 2025

ISBN Information:
Electronic ISBN:979-8-3315-9497-8
Print on Demand(PoD) ISBN:979-8-3315-9498-5

ISSN Information:
Electronic ISSN: 2837-4967
Print on Demand(PoD) ISSN: 2837-4959

Effect of Ag-doping on the photoluminescence of nanostructered ZnS material

Ana Laura Curcio
Institute of Geosciences and Exact Sciences
São Paulo Sate University (Unesp)
Rio Claro – SP, Brazil
https://orcid.org/0000-0003-4750-8592

Thiago Ardana Chaim
Institute of Geosciences and Exact Sciences
São Paulo Sate University (Unesp)
Rio Claro – SP, Brazil
https://orcid.org/0009-0005-8833-7437

Maria Inês Basso Bernardi
São Carlos Institute of Physics
University of São Paulo
São Carlos – SP, Brazil
https://orcid.org/0000-0001-7220-078X

Fabio Simões de Vicente
Institute of Geosciences and Exact Sciences
São Paulo Sate University (Unesp)
Rio Claro – SP, Brazil
https://orcid.org/0000-0001-7696-3004

Adriano José Galvani Otuka
Institute of Geosciences and Exact Sciences
São Paulo Sate University (Unesp)
Rio Claro – SP, Brazil
https://orcid.org/0000-0002-9496-7225

Alexandre Mesquita
Institute of Geosciences and Exact Sciences
São Paulo Sate University (Unesp)
Rio Claro – SP, Brazil
https://orcid.org/0000-0001-8524-0959

2025 SBFoton International Optics and Photonics Conference (SBFoton IOPC) | 979-8-3315-9497-8/25/$31.00 ©2025 IEEE | DOI: 10.1109/SBFOTONIOPC66433.2025.11218612

***Abstract*— Zinc sulfide (ZnS) is a wide band gap semiconductor with numerous technological applications in optical devices. In this study, nanostructured Ag-doped ZnS samples were prepared by solvothermal method. Pure-ZnS sample exhibits cubic symmetry of sphalerite structure whereas samples with higher values of Ag content exhibits coexistence of sphalerite structure and wurtzite structure with hexagonal symmetry. Photoluminescence spectra present typical four emissions ascribed to Zn and S vacancies, Zn and S interstitials for ZnS host matrix. As the Ag content increases, the relative intensity increases for red-orange emissions and an additional emission is observed, allowing a tunable photoluminescence emission with Ag-doping.**

Keywords—ZnS, Zinc sulfide, Ag-doped, silver, photoluminescence, solvothermal method, tunable color.

I. Introduction

II-VI inorganic semiconductors like ZnO, SnO_2, TiO_2, CdS, CdSe, ZnSe, and ZnTe are well-known for their interesting luminescence, magnetic, and electrical properties [1–3]. Among these, zinc sulfide (ZnS) is another notable II-VI inorganic semiconductor. ZnS has garnered significant attention due to its fundamental physical properties, versatility, non-toxicity, chemical stability, and potential for numerous technological applications [1–3]. With a wide band gap ranging from 3.7 to 3.9 eV and a high exciton binding energy of 40 meV, ZnS finds extensive use in various optical devices, including: ultraviolet light-emitting diodes, flat panel display, lasers, photodectors, phosphor in electroluminescent devices, scintillators and solar cells [1–3]. Moreover, ZnS compounds also show activity in the photodegradation of organic materials since trapped holes originated from surface defects on the material.

Given its wide band-gap semiconductor behavior, zinc sulfide (ZnS) readily accommodates various metal ions as luminescent centers, which can improve or modify its structural and optical performance [1–3]. Introducing dopants or impurities creates discrete energy levels within the intrinsic quantum energy levels of ZnS. This, in turn, enhances the host semiconductor's optical, electronic, and magnetic properties. Researchers have successfully incorporated a range of metal ions, including Mn^{2+}, Cu^{2+}, Pb^{2+}, Ag^{+}, Cr^{3+}, Ni^{2+}, and Eu^{2+}, into the ZnS lattice [1–3]. The primary goal of this doping process is to modulate ZnS luminescence properties by forming various energy levels within the band gap of the host matrix.

Therefore, the photoluminescence emission can be tuned and tailored using the appropriated doping ion. Thus, the main aim of this study was to investigate the effect of Ag-doping on the photoluminescent properties of ZnS host material. Samples of Ag-doped ZnS material (ZSA) were prepared using solvothermal method, which stands out as a particularly advantageous route for synthesizing materials like ZnS. It operates at relatively low temperatures and utilizes inexpensive and low-toxicity precursors. This approach also simplifies the incorporation of metal ions, such as silver, into the ZnS lattice.

II. Experimental procedure

In this study, Ag-doped ZnS ($Zn_{1-x}Ag_xS$) nanoparticles, were synthesized with silver concentrations of x = 0.00 (labeled as ZnS), 0.01 (ZSA1), 0.05 (ZSA5) and 0.10 (ZSA10) using a solvothermal method. This approach, essentially based on a chemical co-precipitation at room temperature, offers distinct advantages over other preparation techniques, including precise stoichiometry control, high purity, and excellent homogeneity of the resulting particles [3]. For the synthesis, zinc dichloride ($ZnCl_2$ – Aldrich, 98%), silver nitrate trihydrate ($AgNO_3$ – Aldrich, 99%), and thiourea (H_2NCSNH_2 – Aldrich 99%) were used as reagents. These precursors were dissolved in ethylene glycol ($C_2H_6O_2$– Synth 99.5%). Subsequently, we added a sodium hydroxide solution (NaOH– Vetec, 97%) dropwise before transferring the mixture to a sealed 110 mL Teflon autoclave. The precursor solutions underwent heat treatment at 140 °C for 30 minutes, with a heating rate of 10 °C/min, under constant stirring. Following the heat treatment, the autoclave was allowed to cool naturally to room temperature. Finally, the precipitated powders were washed multiple times with deionized water until a neutral pH was achieved. The powder samples were then dried at 80 °C for 12 hours.

Room-temperature X-ray diffraction (XRD) analysis was performed with measurements using a Rigaku Ultima 4 powder diffractometer. This instrument, configured in a θ−2θ geometry, was equipped with a rotating anode X-ray source emitting Cu-Kα radiation (λ=1.542 Å) and a scintillation

This study was supported by FAPESP (through projects 2013/12993-4 and 2024/22584-9) and CNPq (473568/2013-6 and 314702/2023-7) funding agencies.

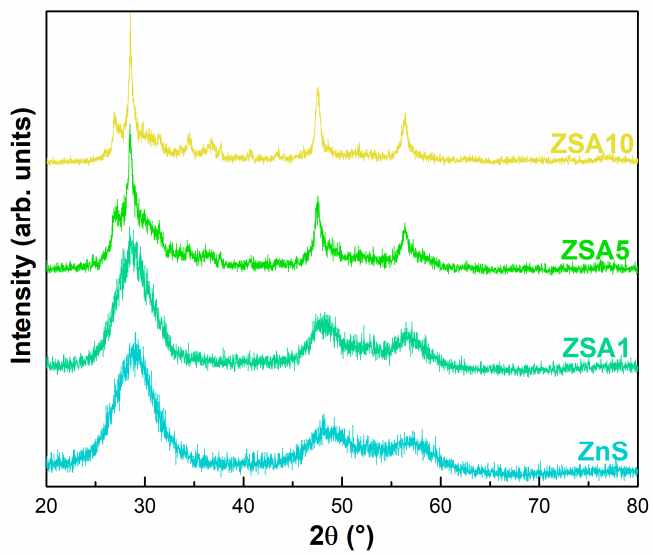

Fig. 1. X-ray diffraction patterns for ZSA samples.

detector. Data were collected with 0.02° step size and a 5-second dwell time per step. We collected room-temperature photoluminescence spectra using a Thermal Jarrel-Ash Monospec monochromator coupled with a Hamamatsu R446 photomultiplier. A krypton ion laser (Coherent Innova), set to an exciting wavelength of 350.6 nm and an output of 200 mW, was used as the excitation source.

III. Results and Discussion

XRD patterns fot ZSA samples are presented in Fig. 1. As can be seen in this Fig., all samples crystallized with broadened diffraction peaks relative to a nanoscaled structure, in agreement with reports at the literature of ZnS based samples prepared with the same route [4]. For ZnS and ZSA1 samples, three peaks are evidently observed at 28.9°, 48.7° and 56.9°, which are indexed to (111), (220) and (311) diffraction planes, respectively, of the sphalerite (zinc blend) structure with *F*-43*m* (216) space group [4]. As the Ag content increases, additional peaks are observed and its intensity is augmented, indicating the coexistence of two crystalline phases at least. The peaks positioned at 26.9°, 28.4°, 30,4°, 38°, 47.6°, 51,6° and 56.5° correspond to (100), (002), (101), (102), (110), (103) and (112) diffraction planes of the wurtzite structure, respectively, with $P6_3mc$ (186) space group [4]. Other peaks with minor intensity are also observed; for example, in the range 32° – 38°, which can be attributed to AgS_2 spurious compound. The results observed in Fig. 1 infer that the incorporation of Ag precursor during synthesis process, as well as the formation of S vacancies due to the heterovalent substitution (Ag^+ for Zn^{2+}), enable the crystallization and nucleation of the wurtzite structure, which is less stable in lower temperatures compared to the sphalerite structure [5],

Photoluminescence spectra for ZnS, ZSA1, ZSA5 and ZSA10 samples are presented in Fig. 2, Fig. 3, Fig. 4 and Fig. 5, respectively. All samples exhibit broad and asymmetrical spectrum, with multiple peaks, suggesting the involvement of various luminescence centers in its radiative processes. In order to understand the ZnS photoluminescence curve, a Gaussian curve fitting were applied, deconvoluting it into four radiative processes, which are labeled as (1), (2) (3) and (4) in Fig. 2 and have been attributed to zinc vacancies (V_{Zn}), sulfur vacancies (V_S), interstitial zinc (Zn_i) and interstitial sulfur (S_i), respectively [3,6].

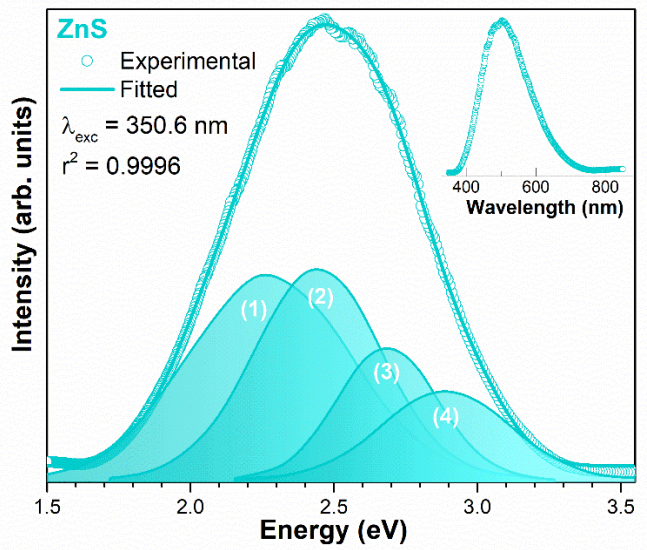

Fig. 2. Photoluminescence spectra for ZnS sample.

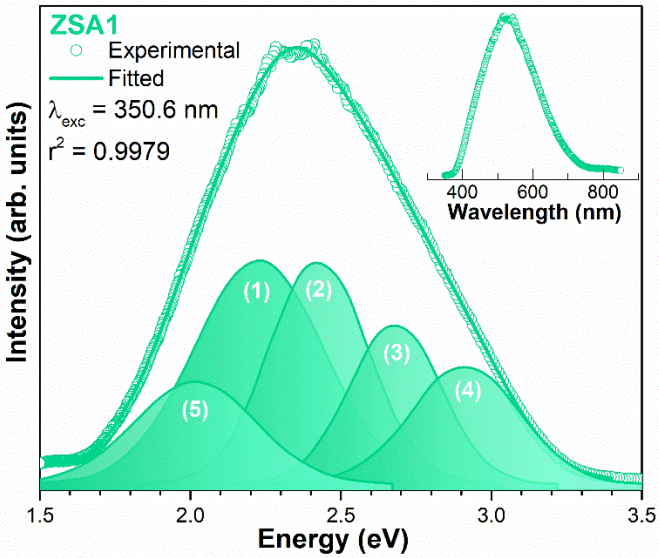

Fig. 3. Photoluminescence spectra for ZSA1 sample.

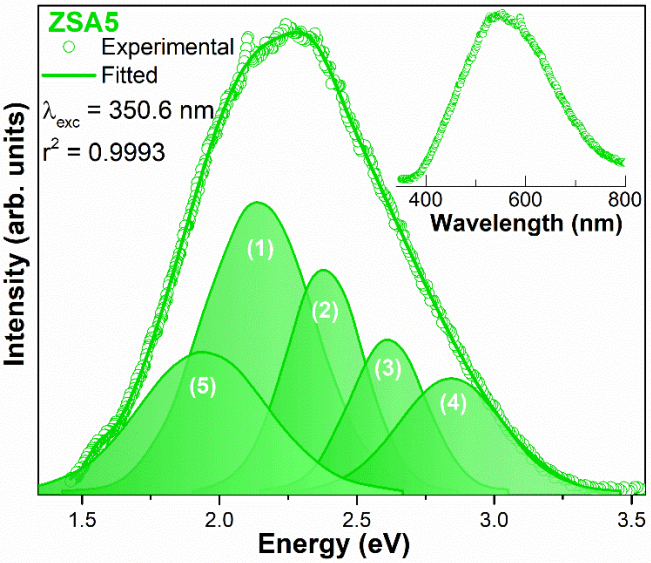

Fig. 4. Photoluminescence spectra for ZSA5 sample.

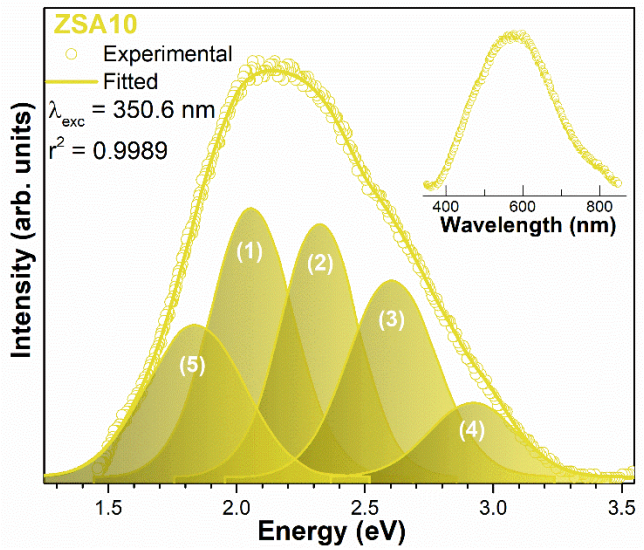

Fig. 5. Photoluminescence spectra for ZSA10 sample.

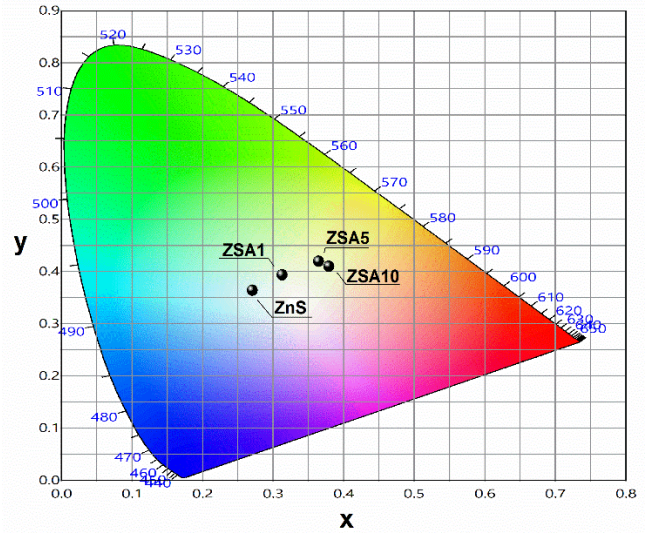

Fig. 6. CIE chromaticity diagram for ZSA samples.

Due to the larger ionic radius of S compared to Zn, interstitial S introduces greater strain, resulting in its electron levels having smaller binding energy and being closer to the valence band than interstitial Zn levels are to the conduction band. Similarly, S vacancy states are nearer the conduction band edge than Zn vacancy states are to the valence band edge [6]. When compared to the photoluminescence spectra reported at the literature, the spectrum in Fig. 2 for ZnS sample shows a red-shift, which is, therefore, likely due to the presence of both sulfur and zinc vacancies [6].

As the Ag^{+} ions are incorporated to the ZnS host matrix, the Gaussian deconvolution is more reliable with an additional peak in orange-red region (labeled as (5)) besides the four emissions in blue-yellow region of the spectra. The position of these four emissions remains practically constant, with an increase of the relative intensity for the emissions ascribed to defects originated by V_{Zn} and V_S. This result is consistent with the fact that the heterovalent substitution of Ag^{+} ions for Zn^{2+} ions induces a formation of V_S. The red-orange emission has been ascribed to a shallow donor-deep acceptor recombination, where the shallow donor center is an Ag ion substituting for Zn and the deep acceptor level is a defect complex at S sites [7].

The CIE coordinates (x, y) [8] for ZSA samples were calculated from the emission spectra and CIE chromaticity diagram and chromaticity coordinates are presented in Fig. 6. As expected for a photoluminescence spectrum composed by four broadened emissions, CIE coordinates for ZnS sample represent bright shades in the blue color emission. As the Ag content increases, the bright shades change into red color direction. This result is explained in terms of the emissions in red-orange region of photoluminescence spectra whose relative intensity is increased with Ag content as depicted in Figs. 3, 4 and 5.

IV. Conclusions

In this study, nanostructured ZSA samples were prepared by solvothermal method. Pure ZnS sample exhibits cubic symmetry of sphalerite structure whereas samples with higher values of Ag content exhibits coexistence of sphalerite structure and wurtzite structure with hexagonal symmetry. Photoluminescence spectra present typical four emissions ascribed to V_{Zn}, V_S, Zn_i and S_i for ZnS host matrix. As the Ag content increases, the relative intensity increases for red-orange emissions and an additional emission is observed, which has been attributed to defects closer de conduction band due to Ag_{Zn}. Thus, tunable photoluminescence emission is observed with Ag-doping, as depicted by CIE coordinates.

References

[1] L. Ralte, K.M.S. Dawngliana, A.L. Fanai, A.L. *et al.* "Effect of ZnS nanoparticles in photoluminescence properties of Tb^{3+} ion doped silica glass for photonic applications," Appl. Phys. A, vol. 129, p. 751, 2023.

[2] S. Mandal, S.I. Ali and A.C. Mandal. "Investigation of structural, optical and photoluminescence properties of the sol–gel synthesized powder ZnS nanoparticles.," Appl. Phys. A, vol. 129, p. 219, 2023.

[3] A.L. Curcio, L.F. Silva, M.I.B. Bernardi, E. Longo and A. Mesquita. "Nanostructured ZnS:Cu phosphor: Correlation between photoluminescence properties and local structure," J. Luminescence, vol. 206, pp. 292-207, 2019.

[4] S. Biswas and S. Kar. "Fabrication of ZnS nanoparticles and nanorods with cubic and hexagonal crystal structures: a simple solvothermal approach," Nanotechnology, vol. 19, p. 045710, 2008.

[5] X. Qian and C. Chen. "Study on theluminescence properties of ZnS:Mn^{2+} particles by high temperature solid phase method," JJ. Phys.: Conf. Ser., vol. 2168, p. 012023, 2022.

[6] R. Kripal, A.K. Gupta, S.K. Mishra, R.K. Srivastava, A.C. Pandey and S.G. Prakash, "Photoluminescence and photoconductivity of ZnS:Mn^{2+} nanoparticles synthesized via co-precipitation method," Spectrochim. Acta Part a-Mol. Biomol. Spectrosc., vol. 76, pp. 523–530, 2010.

[7] Y. Wu, Y. Shao and L.G. Jacobsohn. "Luminescence of ZnS:Ag scintillator prepared by the hydrothermal reaction method: Effects of reaction temperature and time, Ag concentration, and co-doping with Al," Opt. Mater., vol. 107, p. 110015, 2020.

[8] A. Surendran and R. Tintu. "Green innovation: cool white light emission from inorganic ZnS nanoparticles with tunable structural and optical properties," J. Mater. Sci-Mater. El., vol. 35, p. 812, 2024.